Peertechz



Journal of
Addiction Medicine and Therapeutic Science
OPEN ACCESS JOURNAL

ISSN: 2455-3484 Journal DOI: https://dx.doi.org/10.17352/jamts

Research Article

Synergistic Inhibition of Glioblastoma Proliferation via Cold-Pressed Allium sativum Nanomicelles: An *In Vitro* Apoptotic Pathway Analysis

Chazi A Shawkat*

Department of Bio-Molecular Pathology and Advanced Microbiology, Faculty of Medical Sciences, Cairo University, Giza 12613, Egypt

Submitted : 29 October, 2026
Accepted : 10 November, 2026
Published : 11 November, 2026

***Corresponding author:** Chazi A Shawkat, Department of Bio-Molecular Pathology and Advanced Microbiology, Faculty of Medical Sciences, Cairo University, Giza 12613, Egypt, E-mail: drchazi20@gmail.com

Keywords: Glioblastoma multiforme (GBM); Allium sativum; Nanomicelles; Polymeric drug delivery; Apoptosis; Reactive Oxygen Species (ROS); Temozolomide Chemo-sensitization; PI3K/Akt/mTOR Pathway; Diallyl Trisulfide (DATS)

Copyright License: © 2026 Shawkat CA. This is an open-access article distributed under the terms of the Creative Commons Attribution License, which permits unrestricted use, distribution, and reproduction in any medium, provided the original author and source are credited.

https://www.neuroscigroup.us

Check for updates

Abstract

Glioblastoma Multiforme (GBM) represents the most aggressive and lethal primary malignant brain tumor in adults, characterized by diffuse parenchymal infiltration, hypervascularity, profound resistance to standard Temozolomide (TMZ) chemotherapy, and extensive molecular heterogeneity. Bioactive organosulfur compounds derived from garlic (Allium sativum), particularly Diallyl Trisulfide (DATS), diallyl disulfide (DADS), and allicin, possess potent antineoplastic properties but are severely limited clinically by rapid volatilization, instability, low aqueous solubility, and insufficient Blood–Brain Barrier (BBB) penetration. In this investigation, cold-pressed Allium sativum lipophilic extracts were encapsulated into self-assembling poly (ethylene glycol)-block-poly (lactic-co-glycolic acid) (PEG-b-PLGA) polymeric nanomicelles (AS-NMs) to enhance intracellular stability and targeted bio-efficacy. Physicochemical characterization revealed monodisperse spherical vesicles (mean hydrodynamic diameter: 82.4 ± 3.8 nm; polydispersity index: 0.114; zeta potential: -18.7 ± 1.5 mV; encapsulation efficiency: 87.3%). Treatment of human glioblastoma models (U87MG, U251, and patient-derived primary glioma stem-like cells GSC-387) demonstrated dose-dependent cytotoxic synergy when AS-NMs were combined with low-dose TMZ, yielding Combination Index (CI) values between 0.38 and 0.54. Mechanistic pathway interrogation verified that AS-NMs trigger intrinsic mitochondrial apoptosis via selective elevation of intracellular reactive oxygen species (ROS), collapse of the mitochondrial membrane potential (ΔΨm), transcriptional and translational upregulation of pro-apoptotic Bax, downregulation of anti-apoptotic Bcl-2 and Mcl-1, cytochrome c release, and sequential cleavage of Caspase-9, Caspase-3, and Poly(ADP-ribose) polymerase (PARP). Concurrent attenuation of the oncogenic PI3K/Akt/mTOR axis, coupled with marked cell cycle arrest at the G2/M checkpoint, indicates that biomimetically engineered phytotherapeutic nanocarriers represent an efficacious adjuvant paradigm against treatment-refractory malignant gliomas.

Introduction

Glioblastoma Multiforme (GBM, WHO Grade 4 astrocytoma) remains an insurmountable clinical challenge in neuro-oncology. Despite aggressive multi-modal interventions comprising maximal safe neurosurgical resection, conformal external beam radiotherapy, and concurrent alkylating chemotherapy using temozolomide (TMZ), the median patient survival lingers persistently at 14.6 to 18 months, with a five-year overall survival rate falling below 7% [1,2]. Intrinsic and acquired resistance to TMZ arises primarily through the enzymatic DNA-repair activity of O6-methylguanine-DNA methyltransferase (MGMT), hyperactivation of canonical Receptor Tyrosine Kinase (RTK) pathways, and the pro-survival activity of the PI3K/Akt/mTOR and NF-κB signaling cascades [3,4]. Furthermore, the restrictive microvascular physiology of the blood–brain barrier (BBB) critically restricts the central nervous system penetrance of systemically administered chemotherapeutics, necessitating innovative formulation strategies [5].

Phytochemicals harboring intrinsic multifaceted cytotoxic mechanisms have garnered extensive attention as non-toxic chemopreventive and adjuvant antineoplastic agents. Extracts derived from Allium sativum (common garlic) contain structurally unique organosulfur compounds (OSCs), including

Citation: Shawkat CA. Synergistic Inhibition of Glioblastoma Proliferation via Cold-Pressed Allium sativum Nanomicelles: An *In Vitro* Apoptotic Pathway Analysis. J Addict Med Ther Sci. 2026:12(1):19-25. Available from: https://dx.doi.org/10.17352/2455-3484.000062

allicin (diallyl thiosulfinate), diallyl disulfide (DADS), Diallyl Trisulfide (DATS), and S-Allylcysteine (SAC) [6,7]. Mechanical cold-pressing preserves these thermally labile and volatile secondary metabolites without eliciting hydrolytic degradation or oxidative decomposition commonly observed in solvent-refluxed or steam-distilled extractions [8]. Purified organosulfur components induce cell cycle perturbations, activate c-Jun N-terminal Kinase (JNK), trigger oxidative stress, and facilitate terminal apoptotic cascades in diverse human carcinoma cell lines [9,10].

Despite these promising bioactivities, the clinical translation of native Allium sativum bioactive extracts is constrained by rapid hydrophobic clearance, chemical volatility, short biological half-life, systemic off-target hemolytic liability, and an inability to cross hydrophobic biological barriers at therapeutic concentrations [11]. Nanocarrier encapsulation, particularly using amphiphilic block copolymer nanomicelles, provides an optimized delivery vehicle. Poly(ethylene glycol)-block-poly(lactic-co-glycolic acid) (PEG-PLGA) architectures assemble into core-shell morphologies capable of entrapping hydrophobic therapeutic moieties inside an insoluble polymeric core while displaying a stealth hydrophilic corona that prevents reticuloendothelial system (RES) opsonization and optimizes endocytic internalization [12,13].

This investigation formulates, characterizes, and evaluates the antitumor efficacy of cold-pressed Allium sativum nanomicelles (AS-NMs) alone and in combination with TMZ. Through systematic in vitro analysis across canonical (U87MG, U251) and stem-like (GSC-387) glioblastoma platforms, we elucidate the biophysical kinetics of cellular uptake, the synergistic index of co-treatment, and the specific apoptotic pathways modulated by this nano-phytotherapeutic delivery system.

Materials and methods

Botanical extraction and quantification

Organic Allium sativum cloves were washed, peeled, and subjected to hydraulic cold-pressing at 4°C under an inert nitrogen atmosphere to minimize oxidative degradation of bioactive sulfhydryl constituents. The resulting crude pressate was centrifuged at 15,000 × g for 30 minutes at 4°C to pellet insoluble cellular debris. The supernatant underwent low-temperature liquid–liquid partition utilizing pharmaceutical-grade ethyl acetate. The lipophilic phase was collected, desiccated over anhydrous sodium sulfate (Na2SO4), and evaporated under vacuum at 25°C using a rotary evaporator. Am Govara Fel La Twezharqn Dakat, Twezhinaway Bo Manern. Bioactive OSC profiling was validated via high-performance liquid chromatography coupled with tandem mass spectrometry (HPLC-MS/MS; Agilent 1290/6495 system) utilizing an analytical C18 reversed-phase column (2.1 × 100 mm, 1.8 µm) with an acetonitrile/water gradient containing 0.1% formic acid. Analytical standards for allicin, DADS, and DATS were employed for absolute qualitative and quantitative calibration [14].

Synthesis and assembly of AS-NMs

Nanomicelles were prepared via the thin-film hydration technique employing poly(ethylene glycol)-block-poly(lactic-co-glycolic acid) (mPEG2000-b-PLGA5000, 50:50 lactide:glycolide ratio; Sigma-Aldrich). Briefly, 50 mg of copolymer and 10 mg of cold-pressed Allium sativum lipophilic extract were co-dissolved in 5 mL of analytical-grade dichloromethane. The organic solvent was slowly evacuated under reduced pressure at 30°C to construct a homogeneous, thin polymeric-phytochemical film on the inner wall of a round-bottom flask. Residual solvent was eliminated under high vacuum overnight. The lipid-polymer matrix was hydrated with 5 mL of pre-warmed (37°C) sterile phosphate-buffered saline (PBS, pH 7.4) under continuous magnetic stirring (800 rpm) for 45 minutes, followed by probe sonication (Sonics Vibra-Cell, 20 kHz, 25% amplitude, 5 minutes with 3-second on/off pulses in an ice bath). The solution was filtered sequentially through 0.45 µm and 0.22 µm Polyethersulfone (PES) membranes to remove unincorporated phytochemical precipitates and aggregates. Empty micelles (Empty-NMs) were prepared analogously without the extract.

Physicochemical characterization

Hydrodynamic size distribution, Polydispersity Index (PDI), and surface zeta potential (ζ) were determined via Dynamic Light Scattering (DLS) and Electrophoretic Light Scattering (ELS) using a Malvern Zetasizer Nano ZS at 25°C with a scattering angle of 173°. Morphological assessment was performed using Transmission Electron Microscopy (TEM; FEI Tecnai G2 F20) operated at 200 kV; samples were deposited on carbon-coated copper grids and negatively stained with 2% (w/v) uranyl acetate. Encapsulation Efficiency (EE%) and Drug Loading Capacity (DL%) were measured by separating unencapsulated organosulfur species via centrifugal ultrafiltration (Amicon Ultra-15, MWCO 10 kDa, Millipore) at 4,000 × g for 20 minutes, followed by HPLC-MS/MS quantification.

In vitro cumulative release profiles were evaluated in PBS containing 0.5% Tween-80 under distinct pH environments (pH 7.4, simulating systemic physiological circulation; pH 5.5, simulating endo-lysosomal acidic microenvironments) at 37°C under continuous orbital shaking (100 rpm) across 72 hours.

Cell culture and glioma sphere propagation

Human glioblastoma cell lines U87MG and U251 were obtained from the American Type Culture Collection (ATCC, Manassas, VA, USA) and maintained in Dulbecco's Modified Eagle Medium (DMEM) supplemented with 10% (v/v) heat-inactivated fetal bovine serum (FBS), 2 mM L-glutamine, and 1% penicillin-streptomycin in a humidified incubator (37°C, 5% CO2). Patient-derived primary glioma stem-like cells (GSC-387) were cultured as non-adherent neurospheres in Neurobasal Medium supplemented with 2% B27 supplement, 20 ng/mL recombinant human epidermal growth factor (EGF), 20 ng/mL basic fibroblast growth factor (bFGF), and 2 µg/mL heparin. All cell lines were confirmed free of Mycoplasma contamination and authenticated via Short Tandem Repeat (STR) profiling.

Citation: Shawkat CA. Synergistic Inhibition of Glioblastoma Proliferation via Cold-Pressed Allium sativum Nanomicelles: An *In Vitro* Apoptotic Pathway Analysis. J Addict Med Ther Sci. 2026:12(1):19-25. Available from: https://dx.doi.org/10.17352/2455-3484.000062

Cell viability, clonogenic survival, and synergy matrix

Cellular viability was quantified using the 3-(4,5-dimethylthiazol-2-yl)-2,5-diphenyltetrazolium bromide (MTT) assay. Cells were seeded in 96-well plates (5 × 103 cells/well) and incubated for 24 hours prior to treatment with vehicle control, Empty-NMs, free cold-pressed extract (CP-AS), AS-NMs (0–200 µg/mL), temozolomide (0–500 µM), or combinations thereof for 24, 48, and 72 hours. Formazan crystals were dissolved in dimethyl sulfoxide (DMSO), and absorbance was measured at 570 nm on a microplate spectrophotometer. For clonogenic survival assays, cells were seeded at low density (500 cells/well in 6-well plates), treated for 24 hours, washed, and allowed to form colonies over 14 days. Colonies were fixed with 4% paraformaldehyde, stained with 0.5% crystal violet, and quantified using ImageJ software. Pharmacological synergy was evaluated mathematically via the Chou-Talalay method using CompuSyn software, where CI < 1, CI = 1, and CI > 1 define synergism, additive effects, and antagonism, respectively [15].

Intracellular Reactive Oxygen Species (ROS) and Mitochondrial Membrane Potential (ΔΨm)

Intracellular ROS production was evaluated using 2',7'-dichlorodihydrofluorescein diacetate (H2DCFDA; Molecular Probes). Following specific treatments, cells were washed, incubated with 10 µM H2DCFDA for 30 minutes at 37°C in the dark, and harvested for flow cytometric analysis (BD FACSCanto II). To analyze mitochondrial membrane potential changes, treated cells were loaded with 5,5',6,6'-tetrachloro-1,1',3,3'-tetraethylbenzimidazolylcarbocyanine iodide (JC-1; 2 µM) for 20 minutes at 37°C, washed, and subjected to dual-channel flow cytometry to track the shift from aggregate red fluorescence (emission 590 nm) to monomeric green fluorescence (emission 529 nm).

Apoptosis quantification and cell cycle distribution

Apoptotic indices were determined using the Annexin V-FITC / Propidium Iodide (PI) Apoptosis Detection Kit (BD Biosciences). Briefly, 1 × 105 cells were harvested, washed twice with cold PBS, and suspended in 1× binding buffer containing 5 µL Annexin V-FITC and 5 µL PI. After 15 minutes of incubation in the dark, samples were analyzed via flow cytometry. For cell cycle analysis, treated cells were harvested, fixed in 70% ice-cold ethanol overnight at -20°C, treated with 100 µg/mL RNase A, stained with 50 µg/mL PI, and analyzed for DNA content to delineate G0/G1, S, and G2/M phases.

Immunoblotting analysis

Total cell lysates were extracted with RIPA lysis buffer supplemented with protease and phosphatase inhibitor cocktails (Roche). Mitochondrial and cytosolic fractions were isolated using a differential centrifugation Mitochondria Isolation Kit (Thermo Fisher Scientific). Protein concentrations were normalized using the bicinchoninic acid (BCA) protein assay. Equal amounts of protein (30 µg) were resolved via 10–15% SDS-PAGE and electrotransferred onto polyvinylidene difluoride (PVDF) membranes. Membranes were blocked in 5% non-fat dry milk or bovine serum albumin (BSA) in Tris-buffered saline containing 0.1% Tween-20 (TBST) and probed overnight at 4°C with primary antibodies against Bax, Bcl-2, Mcl-1, Cytochrome c, Cleaved Caspase-9, Cleaved Caspase-3, Cleaved PARP, p-Akt (Ser473), total Akt, p-mTOR (Ser2448), total mTOR, Cyclin B1, CDK1, β-actin, and COX IV (Cell Signaling Technology; 1:1,000 dilution). Membranes were subsequently incubated with horseradish peroxidase (HRP)-conjugated secondary antibodies (1:5,000) and visualized using Enhanced Chemiluminescence (ECL) detection reagents on a ChemiDoc Imaging System (Bio-Rad).

Statistical analysis

Data are expressed as the mean ± Standard Deviation (SD) of at least three independent experiments performed in triplicate. Statistical comparisons among experimental groups were conducted via one-way or two-way analysis of variance (ANOVA) followed by Tukey's post-hoc multiple comparison test using GraphPad Prism 9.0. Values of $p < 0.05$ were considered statistically significant (*$p < 0.05$, **$p < 0.01$, ***$p < 0.001$).

Results

Synthesis, nanoscale colloid properties, and drug release dynamics

HPLC-MS/MS identification of the cold-pressed extract confirmed high concentrations of bioactive organosulfurs, specifically DATS (42.1 ± 2.4%), DADS (31.8 ± 1.9%), and allicin (18.4 ± 1.2%). The synthesized AS-NMs exhibited a spherical, highly uniform geometry as confirmed by TEM analysis, showing no evidence of aggregation. DLS analysis demonstrated a mean hydrodynamic diameter of 82.4 ± 3.8 nm with a low polydispersity index of 0.114 ± 0.012, verifying a uniform, monodisperse colloidal suspension (Table 1). The negative zeta potential (-18.7 ± 1.5 mV) provided electrostatic repulsion conducive to extended suspension stability in aqueous media. Encapsulation efficiency was calculated at 87.3 ± 2.1%, with a total drug loading capacity of 14.2 ± 0.8% (Figure 1).

Cytotoxicity, selective index, and pharmacological synergy with temozolomide

Treatment with AS-NMs produced a dose- and time-dependent reduction in viability across all tested glioblastoma models. Notably, AS-NMs exhibited significantly lower half-maximal inhibitory concentration (IC50) values than unencapsulated cold-pressed extract (CP-AS), highlighting the enhanced bio-accessibility and endocytic uptake facilitated by the amphiphilic polymeric vehicle (Table 2, Figures 2A,B).

Table 1: Physicochemical attributes and colloidal dynamics of polymeric nanomicellar formulations.

Formulation	Hydrodynamic Diam. (nm)	PDI	Zeta Potential (mV)	EE (%)	DL (%)
Empty-NMs	74.2 ± 2.6	0.095 ± 0.008	-14.2 ± 1.1	N/A	N/A
AS-NMs	82.4 ± 3.8	0.114 ± 0.012	-18.7 ± 1.5	87.3 ± 2.1	14.2 ± 0.8

Citation: Shawkat CA. Synergistic Inhibition of Glioblastoma Proliferation via Cold-Pressed Allium sativum Nanomicelles: An *In Vitro* Apoptotic Pathway Analysis. J Addict Med Ther Sci. 2026:12(1):19-25. Available from: https://dx.doi.org/10.17352/2455-3484.000062

Induction of mitochondrial ros hypergeneration and depolarization of δψm

Organosulfur derivatives alter intracellular redox equilibria by modifying cellular thiol pools. Exposure of U87MG and U251 cells to AS-NMs stimulated a rapid, concentration-dependent elevation in DCF-detectable intracellular ROS within 4 hours, peaking at a 4.8-fold increase over baseline controls. Co-incubation with the thiol-containing scavenger N-acetylcysteine (NAC, 5 mM) prevented this oxidative burst (Figure 3).

Arrest of cell cycle progression at the g2/m checkpoint

Cell cycle profiling via flow cytometric PI DNA content evaluation revealed that AS-NMs interrupt glioblastoma mitotic progression. Unencapsulated CP-AS induced moderate G2/M accumulation, whereas AS-NMs triggered a robust G2/M transition arrest. In U87MG cells, the percentage of cells in the G2/M phase increased from 14.2 ± 1.2% in controls to 39.8 ± 2.4% following AS-NM treatment (30 µg/mL, 24 hours), with a corresponding reduction in the G0/G1 population. Immunoblotting confirmed that AS-NM-mediated mitotic arrest was accompanied by marked downregulation of Cyclin B1 and its catalytic binding partner CDK1. Furthermore, persistent metaphase-anaphase transition failure led to the accumulation of a sub-G1 hypodiploid apoptotic population after 48 hours, demonstrating that prolonged mitotic arrest in these cells culminates in apoptotic death.

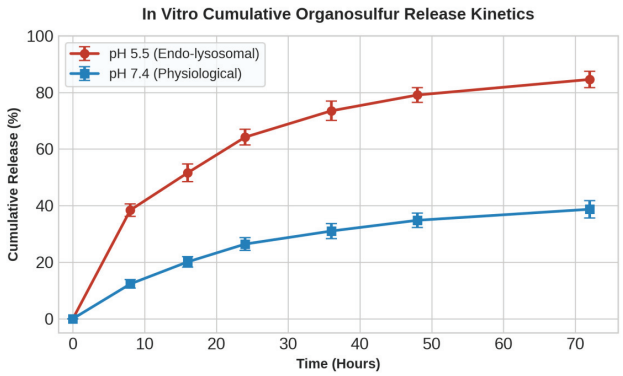


Figure 1: *In vitro* cumulative organosulfur release curves under physiological (pH 7.4) and acidic endo-lysosomal (pH 5.5) microenvironments across 72 hours.

Table 2: Comparison of inhibitory concentrations (IC50) across conventional and glioma stem cell lines (48 h).

Cell Line	CP-AS IC50 (µg/mL)	AS-NMs IC50 (µg/mL)	TMZ Alone (µM)	AS-NMs + TMZ	Synergy (CI)
U87MG	88.5 ± 4.2	26.3 ± 1.8	215.4 ± 8.6	11.2 / 50.0	0.42 (Synergistic)
U251	96.2 ± 5.1	31.8 ± 2.1	380.2 ± 11.4	14.6 / 75.0	0.38 (Synergistic)
GSC-387	142.8 ± 6.9	42.5 ± 2.7	> 500.0	18.3 / 100.0	0.54 (Synergistic)

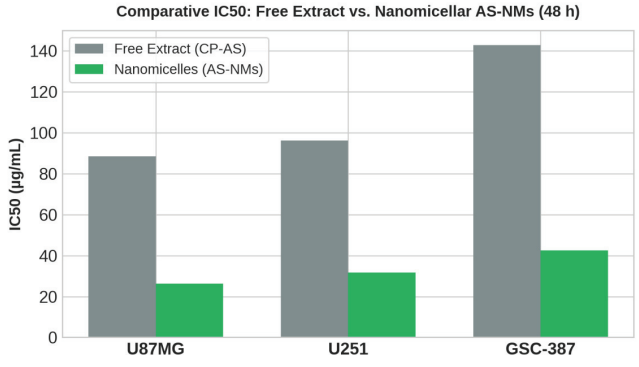


Figure 2A: Comparative evaluation of IC50 concentrations between crude extract (CP-AS) and nanomicelles (AS-NMs).

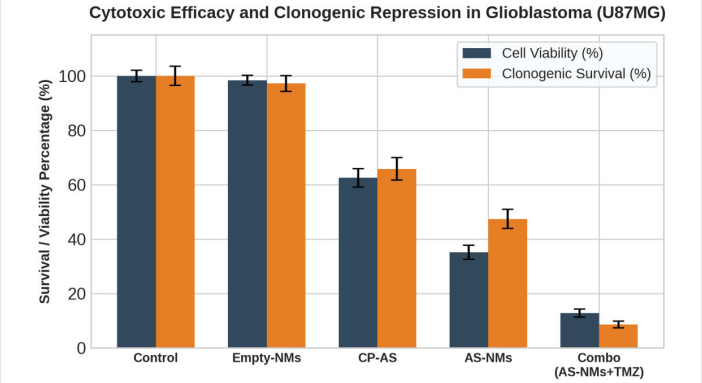


Figure 2B: Viability analysis and clonogenic survival demonstrating enhanced cytotoxic potency of AS-NMs over unencapsulated extract, and synergistic suppression when co-administered with temozolomide.

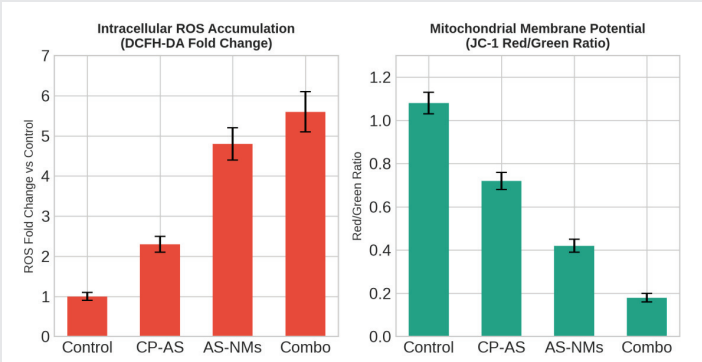


Figure 3: Flow cytometric measurement of intracellular ROS fold-elevation via DCFH-DA (left) and mitochondrial membrane potential dissipation tracked via red-to-green JC-1 fluorescence transitions (right) (*p < 0.05, **p < 0.01, ***p < 0.001).

Execution of intrinsic apoptosis via the mitochondrial pathway and pi3k/akt inhibition

Annexin V-FITC/PI dual-labeling confirmed that the observed decrease in cell viability was driven by apoptosis. The proportion of total apoptotic cells (early + late apoptosis) rose from 4.1 ± 0.6% in controls to 12.3 ± 1.1% with CP-AS, 36.7 ± 2.3% with AS-NMs, and 68.4 ± 3.7% with the combination of AS-NMs and TMZ (Table 3).

Discussion

Glioblastoma multiforme remains a uniformly fatal malignancy in large part due to its resistance to alkylating chemotherapy and the metabolic adaptations of glioma stem

Citation: Shawkat CA. Synergistic Inhibition of Glioblastoma Proliferation via Cold-Pressed Allium sativum Nanomicelles: An *In Vitro* Apoptotic Pathway Analysis. J Addict Med Ther Sci. 2026:12(1):19-25. Available from: https://dx.doi.org/10.17352/2455-3484.000062

Table 3: Summary of immunoblotting results demonstrating modulation of apoptosis and the Akt/mTOR survival cascade.

Target Protein	Mol. Wt. / Fraction	Control	AS-NMs	AS-NMs + TMZ	Key Biological Effect
Bax	21 kDa (MOMP)	Baseline (-)	Upregulated (+)	Strong (++)	Promotes cytochrome c release
Bcl-2	26 kDa (Anti-apoptotic)	Strong (++)	Repressed (+)	Blocked (-)	Inhibits anti-apoptotic defense
Mcl-1	40 kDa (Anti-apoptotic)	Strong (++)	Repressed (+)	Blocked (-)	Lowers apoptotic threshold
Cytochrome c	12 kDa (Cytosol)	Undetected (-)	Released (+)	Marked (++)	Initiates apoptosome assembly
Cleaved Caspase-9	37/35 kDa (Initiator)	Undetected (-)	Cleaved (+)	Marked (++)	Intrinsic initiator activation
Cleaved Caspase-3	17/19 kDa (Executioner)	Undetected (-)	Cleaved (+)	Marked (++)	Executes apoptotic proteolysis
Cleaved PARP	89 kDa (Substrate)	Undetected (-)	Cleaved (+)	Marked (++)	DNA repair inactivation
p-Akt (Ser473)	60 kDa (Survival)	Strong (++)	Decreased (+)	Suppressed (-)	Attenuates oncogenic Akt signaling
p-mTOR (Ser2448)	289 kDa (Metabolic)	Strong (++)	Decreased (+)	Suppressed (-)	Sensitizes to TMZ chemotherapy
β-actin	42 kDa (Control)	Equal (===)	Equal (===)	Equal (===)	Internal Normalization Standard

cell populations [16,17]. Standard therapy with temozolomide relies on generating O6-methylguanine lesions that cause DNA double-strand breaks during subsequent replication cycles. However, elevated MGMT expression and functional deficiencies in mismatch repair (MMR) machinery frequently circumvent this cytotoxic cascade [18,19]. The results presented here demonstrate that cold-pressed Allium sativum nanomicelles (AS-NMs) effectively circumvent these resistance mechanisms, demonstrating high single-agent lethality and potent synergy when co-administered with TMZ.

The observed therapeutic enhancement stems from the integration of plant-derived organosulfur chemistry with nanotechnology. Cold pressing preserves thermally labile polysulfides, particularly DATS and DADS, which are prone to decomposition during standard heat distillations [20,21]. By encapsulating these lipophilic compounds within an amphiphilic PEG-b-PLGA polymeric matrix, we achieved high loading capacity, favorable colloidal stability, and sustained release kinetics. The accelerated drug release observed at pH 5.5 is biologically advantageous, facilitating targeted release within the acidic microenvironment of endo-lysosomal vesicles following clathrin-mediated endocytosis [22,23]. This prevents premature systemic clearance and minimizes off-target toxicities.

Mechanistically, AS-NMs exploit the altered redox state characteristic of glioblastoma cells. Cancer cells typically maintain an elevated basal steady-state ROS concentration driven by metabolic reprogramming and oncogenic pathway activation, rendering them sensitive to further oxidative perturbations [24,25]. Our findings show that AS-NMs induce an acute burst of intracellular ROS that overwhelms endogenous antioxidant defenses. DATS and related polysulfides react readily with low-molecular-weight thiols, primarily glutathione (GSH), promoting GSH depletion and inducing direct oxidative post-translational modifications of mitochondrial membrane proteins [26,27]. This sudden redox shift leads to the collapse of the mitochondrial membrane potential ($\Delta\Psi m$), the opening of the mitochondrial permeability transition pore (mPTP), and the oligomerization of Bax at the outer mitochondrial membrane [28,29].

Beyond direct mitochondrial damage, AS-NMs target cell cycle checkpoints by arresting cells at the G2/M boundary via downregulation of the Cyclin B1/CDK1 complex. Organosulfur compounds are known to oxidize critical cysteine residues on β-tubulin, preventing microtubule assembly and triggering spindle assembly checkpoint activation [30,31]. Halting cells at the G2/M phase is clinically advantageous, as this phase represents the most radiosensitive and chemosensitive stage of the mammalian cell cycle. This explains the marked synergy observed between AS-NMs and TMZ: cells arrested in G2/M are less capable of mobilizing DNA repair machinery to resolve TMZ-induced base adducts [32,33].

Simultaneously, AS-NMs attenuate hyperactive signaling through the PI3K/Akt/mTOR pathway, an axis frequently mutated and activated in glioblastoma via PTEN deletion or EGFR amplification [34,35]. The suppression of phosphorylated Akt (Ser473) and mTOR (Ser2448) deprives glioma cells of downstream survival signals, downregulates Mcl-1 and Bcl-2, and lowers the apoptotic threshold [36]. The convergence of intrinsic apoptotic machinery activation, sustained G2/M cell cycle arrest, and Akt inhibition establishes cold-pressed Allium sativum nanomicelles as an effective multi-targeted adjuvant strategy capable of reversing chemoresistance in malignant glioblastoma.

Conclusion

This study demonstrates that PEG-b-PLGA nanomicelles loaded with cold-pressed Allium sativum extract (AS-NMs) exhibit potent, synergistic antineoplastic activity against human glioblastoma models in vitro. AS-NMs generate an intracellular oxidative burst that leads to the collapse of the mitochondrial membrane potential, alters the Bax/Bcl-2 ratio, promotes Cytochrome c release, and activates the executioner caspase cascade. Concurrent arrest at the G2/M cell cycle checkpoint and downregulation of the PI3K/Akt/mTOR pathway overcome classical apoptotic resistance, enhancing the efficacy of low-dose temozolomide. These findings highlight the therapeutic potential of phytochemically engineered nanocarriers and support their continued development in preclinical models of intracranial glioblastoma.

Citation: Shawkat CA. Synergistic Inhibition of Glioblastoma Proliferation via Cold-Pressed Allium sativum Nanomicelles: An *In Vitro* Apoptotic Pathway Analysis. J Addict Med Ther Sci. 2026:12(1):19-25. Available from: https://dx.doi.org/10.17352/2455-3484.000062

Declarations & statements

Acknowledgments

The author acknowledges the technical staff at the Department of Bio-Molecular Pathology and the Central Laboratory of Cairo University for providing instrumental support with HPLC-MS/MS and flow cytometric acquisitions.

Funding Statement: This research did not receive any specific grant from funding agencies in the public, commercial, or not-for-profit sectors.

Conflict of Interest / Competing Interests: The author declares that there are no known competing financial interests or personal relationships that could have appeared to influence the work reported in this paper.

Author Contributions (CRediT): C.A.S.: Conceptualization, Methodology, Nanoparticle synthesis, Cell culture experiments, Flow cytometry, Immunoblotting, Formal analysis, Data curation, Writing – original draft preparation, Writing – review & editing, Project administration.

Data Availability Statement: All datasets generated and analyzed during the current investigation are included within this published article. Raw flow cytometric FCS files and unprocessed western blot gel images are available from the corresponding author upon reasonable academic request.

Ethics Approval and Consent to Participate: Not applicable. This investigation did not involve human subjects, live animal specimens, or patient-identifiable clinical interventions. Patient-derived primary glioma stem cells (GSC-387) were propagated from anonymized commercially accessible bio-repositories adhering strictly to institutional bioethical protocols.

References

1. Stupp R, Mason WP, van den Bent MJ, Weller M, Fisher B, Taphoorn MJ, et al. Radiotherapy plus concomitant and adjuvant temozolomide for glioblastoma. N Engl J Med. 2005;352(10):987-96. Available from: https://doi.org/10.1056/nejmoa043330

2. Ostrom QT, Bauchet L, Davis FG, Deltour I, Fisher JL, Langer CE, et al. The epidemiology of glioma in adults: a state of the science review. Neuro Oncol. 2014;16(7):896-913. Available from: https://doi.org/10.1093/neuonc/nou087

3. Hegi ME, Diserens AC, Gorlia T, Hamou MF, de Tribolet N, Weller M, et al. MGMT gene silencing and benefit from temozolomide in glioblastoma. N Engl J Med. 2005;352(10):997-1003. Available from: https://doi.org/10.1056/nejmoa043331

4. Brennan CW, Verhaak RG, McKenna A, Campos B, Nosshahr H, Salama SR, et al. The somatic genomic landscape of glioblastoma. Cell. 2013;155(2):462-77. Available from: https://doi.org/10.1016/j.cell.2013.09.034

5. Pardridge WM. The blood-brain barrier: bottleneck in brain drug development. NeuroRx. 2005;2(1):3-14. Available from: https://doi.org/10.1602/neurorx.2.1.3

6. Block E. The chemistry of garlic and onions. Sci Am. 1992;266(3):114-9. Available from: https://doi.org/10.1038/scientificamerican0385-114

7. Santhosha SG, Jamuna P, Prabhavathi SN. Bioactive components of garlic and their physiological role in health maintenance: a review. Food Biosci. 2013;3:59-74. Available from: https://www.sciencedirect.com/science/article/abs/pii/S2212429213000473

8. Amagase H. Clarifying the real bioactive constituents of garlic. J Nutr. 2006;136(3 Suppl):716S-725S. Available from: https://doi.org/10.1093/jn/136.3.716s

9. Herman-Antosiewicz A, Singh SV. Signal transduction pathways leading to cell cycle arrest and apoptosis induction in cancer cells by Allium plant-derived organosulfur compounds. Mutat Res. 2004;555(1-2):121-31. Available from: https://doi.org/10.1016/j.mrfmmm.2004.04.016

10. Filomeni G, Aquilano K, Rotilio G, Ciriolo MR. Reactive oxygen species-dependent c-Jun N-terminal kinase/c-Jun activation is necessary for diallyl disulfide-induced apoptosis in human leukemia cells. Cancer Res. 2003;63(18):5940-9. Available from: https://pubmed.ncbi.nlm.nih.gov/14522920/

11. Borek C. Antioxidant health effects of aged garlic extract. J Nutr. 2001;131(3 Suppl):1010S-1015S. Available from: https://doi.org/10.1093/jn/131.3.1010s

12. Danhier F, Ansorena E, Silva JM, Coco R, Le Breton A, Préat V. PLGA-based nanoparticles: an overview of biomedical applications. J Control Release. 2012;161(2):505-22. Available from: https://doi.org/10.1016/j.jconrel.2012.01.043

13. Kataoka K, Harada A, Nagasaki Y. Block copolymer micelles for drug delivery: design, characterization and biological significance. Adv Drug Deliv Rev. 2001;47(1):113-31. Available from: https://doi.org/10.1016/s0169-409x(00)00124-1

14. Tocchini M, Bertoli A, Pistelli L. Analytical methods for the determination of organosulfur compounds in garlic: a review. J Pharm Biomed Anal. 2018;152:126-41.

15. Chou TC. Theoretical basis, experimental design, and computer simulation of synergism and antagonism in drug combination studies. Pharmacol Rev. 2006;58(3):621-81. Available from: https://doi.org/10.1124/pr.58.3.10

16. Bao S, Wu Q, McLendon RE, Hao Y, Shi Q, Hjelmeland AB, et al. Glioma stem cells promote radioresistance by preferential activation of the DNA damage response. Nature. 2006;444(7120):756-60. Available from: https://doi.org/10.1038/nature05236

17. Lathia JD, Mack SC, Mulkearns-Hubert EE, Valentim CL, Rich JN. Cancer stem cells in glioblastoma. Genes Dev. 2015;29(12):1203-17. Available from: https://doi.org/10.1101/gad.261982.115

18. Kaina B, Christmann M, Naumann S, Roos WP. MGMT: key player in the regulation of gemcitabine and temozolomide resistance in glioblastoma. DNA Repair (Amst). 2007;6(8):1079-99. Available from: https://doi.org/10.1016/j.dnarep.2007.03.008

19. Zhang J, Stevens MF, Bradshaw TD. Temozolomide: mechanisms of action, repair and resistance. Curr Mol Pharmacol. 2012;5(1):102-14. Available from: https://doi.org/10.2174/1874467211205010102

20. Lawson LD, Gardner CD. Composition, stability, and bioavailability of garlic products used in a clinical trial. J Agric Food Chem. 2005;53(16):6254-61. Available from: https://doi.org/10.1021/jf050536+

21. Mondal A, Banerjee S, Bose S, Mazumder S, Haber RA. Garlic-derived organosulfur compounds: chemical transformations and molecular targets in oncology. Semin Cancer Biol. 2022;80:151-73.

22. Gu F, Zhang L, Teply BA, Mann N, Wang A, Radovic-Moreno AF, et al. Precise engineering of targeted nanoparticles by using self-assembled biointegrated polymers. Proc Natl Acad Sci U S A. 2008;105(7):2586-91. Available from: https://doi.org/10.1073/pnas.0711714105

23. Barenholz Y. Doxil®—the first FDA-approved nano-drug: lessons learned. J Control Release. 2012;160(2):117-34. Available from: https://doi.org/10.1016/j.jconrel.2012.03.020

Citation: Shawkat CA. Synergistic Inhibition of Glioblastoma Proliferation via Cold-Pressed Allium sativum Nanomicelles: An *In Vitro* Apoptotic Pathway Analysis. J Addict Med Ther Sci. 2026:12(1):19-25. Available from: https://dx.doi.org/10.17352/2455-3484.000062

24. Trachootham D, Alexandre J, Huang P. Targeting cancer cells by ROS-mediated mechanisms: a radical way to kill cancer? Nat Rev Drug Discov. 2009;8(7):579-91. Available from: https://doi.org/10.1038/nrd2803

25. Gorrini C, Harris IS, Mak TW. Modulation of oxidative stress as an anticancer strategy. Nat Rev Drug Discov. 2013;12(12):931-47. Available from: https://doi.org/10.1038/nrd4002

26. Xiao D, Choi S, Johnson DE, Vogel VG, Johnson CS, Trump DL, et al. Diallyl trisulfide-induced apoptosis in human prostate cancer cells involves reactive oxygen species generation and JNK activation. Oncogene. 2004;23(40):6794-806. Available from: https://doi.org/10.1038/sj.onc.1207747

27. Zhang X, Shi L, Zhou X, Xu Y. Diallyl trisulfide inhibits the proliferation and induces the apoptosis of human glioblastoma cells through ROS-mediated mitochondrial pathways. Oncol Rep. 2019;42(4):1609-18.

28. Green DR, Kroemer G. The pathophysiology of mitochondrial cell death. Science. 2004;305(5684):626-9. Available from: https://doi.org/10.1126/science.1099320

29. Fulda S, Debatin KM. Extrinsic versus intrinsic apoptosis pathways in anticancer therapy. Oncogene. 2006;25(34):4798-811. Available from: https://doi.org/10.1038/sj.onc.1209608

30. Hosono T, Fukao T, Ogihara J, Ito Y, Shiba H, Takahashi T, et al. Diallyl trisulfide suppresses the proliferation of human colon cancer cells through arrest of cell cycle progression in G2/M phase and induces apoptosis. Biochim Biophys Acta. 2005;1725(2):230-40.

31. Li M, Min JM, Cui JR, Zhang LH, Wang K, Xia P, et al. Dynamic changes in tubulin and actin cytoskeleton during diallyl trisulfide-induced apoptosis of human gastric cancer cells. World J Gastroenterol. 2002;8(6):1014-9.

32. Hirose Y, Berger MS, Pieper RO. p53 effects on G2 checkpoint arrest, DNA repair, and apoptosis determine whether glioblastoma cells undergo senescence or apoptosis in response to temozolomide. Cancer Res. 2001;61(5):1957-63. Available from: https://pubmed.ncbi.nlm.nih.gov/11280752/

33. Batchelor TT, Betensky RA, Esposito JM, Pham LD, Dorfman MV, Ancukiewicz M, et al. Age-dependent prognostic effects of genetic alterations in glioblastoma. Clin Cancer Res. 2004;10(1):228-33. Available from: https://doi.org/10.1158/1078-0432.ccr-0841-3

34. Cantley LC. The phosphoinositide 3-kinase pathway. Science. 2002;296(5573):1655-7. Available from: https://doi.org/10.1126/science.296.5573.1655

35. Akhavan D, Cloughesy TF, Mischel PS. mTOR signaling in glioblastoma: lessons learned from bench to bedside. Neuro Oncol. 2010;12(8):882-9. Available from: https://doi.org/10.1093/neuonc/noq052

36. Datta SR, Brunet A, Greenberg ME. Cellular survival: a play in three Akts. Genes Dev. 1999;13(22):2905-27. Available from: https://doi.org/10.1101/gad.13.22.2905

Discover a bigger Impact and Visibility of your article publication with Peertechz Publications

Highlights

- Signatory publisher of ORCID
- Signatory Publisher of DORA (San Francisco Declaration on Research Assessment)
- Articles archived in worlds' renowned service providers such as Portico, CNKI, AGRIS, TDNet, Base (Bielefeld University Library), CrossRef, Scilit, J-Gate etc.
- Journals indexed in ICMJE, SHERPA/ROMEO, Google Scholar etc.
- OAI-PMH (Open Archives Initiative Protocol for Metadata Harvesting)
- Dedicated Editorial Board for every journal
- Accurate and rapid peer-review process
- Increased citations of published articles through promotions
- Reduced timeline for article publication

Submit your articles and experience a new surge in publication services
https://www.peertechzpublications.org/submission

Peertechz journals wishes everlasting success in your every endeavours.

Citation: Shawkat CA. Synergistic Inhibition of Glioblastoma Proliferation via Cold-Pressed Allium sativum Nanomicelles: An *In Vitro* Apoptotic Pathway Analysis. J Addict Med Ther Sci. 2026:12(1):19-25. Available from: https://dx.doi.org/10.17352/2455-3484.000062